A Graph Convolutional Network for Detecting Parkinson's Disease Using Functional Connectivity from fMRI - ECE 228

Aryan Agarwal
Electrical and Computer Engineering
ara005@ucsd.edu

Udit Iyengar
Electrical and Computer Engineering
uiyengar@ucsd.edu

Rommani Mondal
BioEngineering
rmondal@ucsd.edu

Abstract

Parkinson's is one of the largest neurological disorders in the world characterized by cognitive and motor impairment. The standard method to diagnose Parkinson's is analyzing structural MRI images of the brain. However, MRI images alone do not provide the level of sensitivity to characterize functional interactions in the brain that distinguish between different neurological disorders. The proposed project aims to develop a graph convolutional neural network to perform disease state classification on a Parkinson's patient from the reconstructed functional connectivity of the brain using a fMRI dataset. The approach includes segmenting the brain with K-means clustering and SynthSeg and generating a graph from BOLD signals at each labeled brain region. In the neural network, a series of convolution layers then extracts relevant features for classification from the graph. To optimize performance and efficiency of the neural network when training on over 91 fMRI images, hyperparameters influencing graph construction, training, and the convolution architecture were optimized to result in 78.95% validation accuracy. Then, when experimenting with a smaller number of parcellations, the validation accuracy increased to over 88%. When a residual GCN model from literature to classify schizophrenia was implemented, the model was optimized from baseline parameters to achieve 84% validation accuracy. This provides better understanding into the considerations of designing a GCN neurological disease classifier and further insight into the characteristics of the functional connectivity associated with Parkinson's. The Colab link is `https://colab.research.google.com/drive/1l5EFqb-xh2ayRcssIeq52JS61rSd22Fq?usp=sharing`.

1 Introduction

Parkinson's disease is a neurodegenerative disorder that affects over 10 million people in the world [1]. The risk of Parkinson's increases with age, and with no cure, the disease impacts people for the rest of their lives with motor impairment symptoms such as tremors, instability, and a general presence of uncontrollable movements. Additionally, the long term effects of Parkinson's translate to certain levels of cognitive impairment, including more serious levels of dementia beyond 10 years of disease [2]. As a standard practice for diagnosing Parkinson's, doctors rely on structural magnetic resonance imaging (MRI) techniques. These MRI images provide doctors with the necessary structural characteristics of a patient's brain to distinguish between a normal or diseased state. However, since structural changes do not explain how characteristic symptoms are manifested, the pathophysiology and brain network

state of Parkinson's disease is better understood and distinguished from other neurodegenerative disorders by analyzing the functional network activity [3], [11].

Functional connectivity is the temporal coherence of anatomically distinct brain regions and quantifies the relationship between measures of neuronal activity from these regions. The Blood-Oxygenation-Level-Dependent (BOLD) signals in resting-state functional MRI (fMRI) images at each pixel location can be used as a marker of neuronal activity to compute a functional connectome [4]. The field of neuroscience has established that the brain can be represented as a graph with nodes representing brain regions connected by edges reflecting functional connections [7]. We aim to explore whether a model can learn a characteristic functional connectivity pattern in Parkinson's disease.

The resulting graph-structured time series of BOLD signals in each brain region represents both the spatial and temporal information that existing networks fail to consider. As such, a novel information processing technique is needed to address the correlation of the functional interactions. By doing so, an adjacency matrix can be created where each pixel represents two spatial brain region nodes, and the value of that pixel represents the edge weight according to temporal dynamics. This generates a functional connectivity graph upon which a spatio-temporal graph convolutional network can derive graph-level predictions [5]. We apply a convolutional network on custom-generated brain graphs to classify whether a patient's functional connectivity is consistent with that of Parkinson's disease.

2 Related Works

Generating a functional connectome and a holistic mapping of the brain that capture the intricacies of neurodegenerative disease remains a significant obstacle in neuroscience. The parcellation method is a fundamental step in generating a graphical representation of functional connectivity from fMRI data. Various methods of segmenting brain regions from MRI exist, of which there are novel ML-based generative models. For instance, SynthSeg was recently introduced as the first U-Net architecture based deep learning model that maintains generalizability when segmenting heterogeneous clinical brain scans [6]. More traditional segmentation methods include K-means clustering, dictionary learning, independent component analysis to generate a mask for images [8]. Moreover, the most standard segmentation method is to apply a co-registered atlas mask with defined anatomical regions. Though it should be noted that the latter is less feasible with experimental data sets for machine learning as the co-registration process requires manually aligning the MRI scan of every subject with the atlas template, which itself is typically customized for a set of study participants. Hence, an exploration of segmentation methods for brain MRI data in machine learning applications is warranted.

Recently, graph neural networks (GNNs) have extended graph learning to network neuroscience and connectomics. The benefit of learning on a wide range of graphs while preserving topological properties has enabled GNNs to expand from morphological to functional and structural brain graph tasks using MRI images. As seen in Figure 1, the recent landscape of GNN-based methods for brain state classification is still relatively new with a total of 14 models published in the past 6 years [7]. Despite over half of the studies focusing on disease classification, the variety of architectures remain limited, especially in classifying Parkinson's disease. Furthermore, existing machine learning methods have been more focused on morphological MRI features of brain tissue which do not capture changes in neuronal activity over time that significantly contribute to brain graph connectivity. One study developed a residual GCN model to diagnose and classify schizophrenia patients based on brain connectivity features from fMRI images. Although the model achieved over 92% accuracy, the study does not suggest the application of the model across various neurological disorders [9]. A component of our experimentation involved training and validating the GCN model described in the study on a Parkinson's disease dataset to better understand the considerations of designing a GCN model for a particular neurological disorder [9].

3 Methods

Before implementing a learning task, each patient's brain needed to be segmented into regions from which the corresponding BOLD signals would be extracted. Since the fMRI images store spatio-temporal data, modeling the connectome as a graph-like structure enables the functional interactions and connectivity strength between brain regions to be represented as nodes and edge

weights, respectively. Significant changes in the functional activity patterns of the graph network can be fed into the learning task to distinguish regional activity patterns between the normal and disease states. The overall process from fMRI segmentation to disease classification is outlined in Figure 1.

As established previously, various segmentation modalities exist in the literature. To understand the utility of parcellation methods on fMRI and anatomical MRI images, we experimented with K-means clustering and SynthSeg respectively during the data preprocessing stage as seen in Figure 3. The goal was to divide the data into a predefined number of regions to represent the nodes of the functional connectome. K-means clustering segments the image by initializing K clusters and then assigning every spatial location in the image to the cluster with the nearest mean [8]. This ensures that for each K segmented brain region, spatial data points in a cluster are allocated according to similar features. On the other hand, SynthSeg implemented a pretrained deep learning model for segmentation according to the true anatomical regions of the brain [6]. Then, the Nilearn Python library applies a mask to extract the BOLD signal time-series from the fMRI images for each segmented brain region into an 300 x N array where N is the number of features and each column contains the 1D time series for a feature. The entire time series array is passed through the *ConnectivityMeasure* Nilearn function to compute a functional connectivity adjacency matrix that captures the edge weights between features.

The adjacency matrix represented the graph structure in an N x N format that could then be passed through our custom-designed GCN model shown in Figure 4. A GCN architecture consisting of three hidden layers with a [GraphConv-BatchNorm-ReLU] structure, followed by a 64 x 1 fully connected layer and a sigmoid function was implemented to generate a binary disease classifier. Through the GraphConv component, each layer performed a convolutional operation to capture the edge weights between nodes and feed forward into the next layer. Before passing through the fully connected layer, a global mean pool was applied to the output of the final hidden layer.

The output from the sigmoid function provided the network with the disease classifying prediction scores for which the gradient of the binary cross entropy (BCE) loss was used to perform backpropagation and improve the learning weights of the model as shown below.

$$BCE = -\frac{1}{N}\sum_{i=0}^{N} y_i \cdot log(\hat{y}_i) + (1 - y_i) \cdot log(1 - \hat{y}_i) \qquad h_i^{(l+1)} = \sigma(b^{(l)} + \sum_{j \in \mathcal{N}(i)} \frac{1}{c_{ji}} h_j^{(l)} W^{(l)})$$

The GCN model was conventionally trained with iterations corresponding to a number of chosen epochs. BCE was used to assess the training and validation performance. Our first experiment involved optimizing the performance of the model by modifying the baseline hyperparameters and architecture of the GCN model to effectively capture the generated graph networks. Once we retrieved the optimized performance and GCN architecture, we experimented with further optimizing the model with a smaller number of brain segments to understand the effects of brain parcellation techniques on performance. Lastly, we implemented a residual GCN model from literature used on another neurological disorder to provide further insights into Parkinson's disease.

4 Results

The dataset used for the following experiments was accessed from OpenNeuro, a free and open neuroimaging study and dataset platform. The dataset consists of resting state fMRI images of healthy and Parkinson's patients corresponding to 50 healthy and 51 disease fMRI images, each consisting of three cross-sectional images [10]. The images are in a Neuroimaging Informatics Technology Initiative (.nii) file format commonly used for MRI data and images. All training was performed with an 80-20 train-test data split. The following are the experiments performed with the model:

4.1 Hyperparameter and Architecture Optimization from the Baseline Model

After implementing the model, we ran it with the fMRI dataset to obtain baseline values for training and validation accuracies and losses. This was done with a corresponding baseline architecture and fixed hyperparameters comprising the values seen in Table 1. These hyperparameter settings yielded the plots for training and validation accuracies and losses shown in Figure 5. After multiple runs, the best values retrieved were a validation accuracy of 58% and loss of 1.4.

Table 1: Initial (Baseline) Hyperparameters

Graph Complexity	20
Batch Size	32
Hidden Channels	128
Threshold	0.5
Learning Rate	1e-2
Epochs	10

From here, the goal of this experiment was to optimize the model to further improve the respective accuracies and losses. To do this, the architecture was first adjusted. We found through experimentation that adding another layer to the base model for a total of 4 layers and adding a Dropout regularization layer resulted in the best relative results. This resulted in accuracy and loss plots seen in Figure 6 where the best values retrieved were a validation accuracy of 73.68% and loss of 0.8086.

Afterwards, the hyperparameters were kept constant and the next step was to optimize the hyperparameters. Through experimentation, we found that reducing the learning rate to 1e-3, the batch size to 22, and increasing the threshold to 0.6 gave the best final optimized version of the model as seen in Figure 7. The best values retrieved were a validation accuracy of 78.95% and loss of 0.7442.

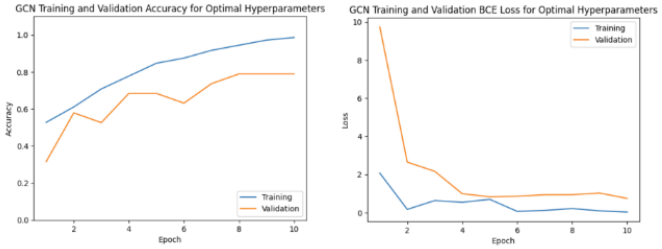

Figure 1: Training and Validation Performance with Optimized Architecture and Hyperparameters

Thus, the optimized model as found through this experiment contains 4 layers in the network structure with dropout regularization, and specified hyperparameters from Table 2.

Table 2: Optimized Hyperparameters

Graph Complexity	20
Batch Size	22
Hidden Channels	128
Threshold	0.6
Learning Rate	1e-3
Epochs	10

4.2 Segmentation Method Analysis

The next experiment analyzed characteristics of different segmentation methods to see how differences in data processing impact the performance of the network model. Additionally, we also aimed to study how changes to the complexity of data passed into the network could impact the final results. We compared SynthSeg segmentation with our K-means clustering implementation used for the resulting model from Experiment 1. Previous versions of the model used 50 parcellations in the segmentation stage, signifying 50 features of the brain for which data was extracted into nodes. However, for this experiment, this was reduced to 32 features to allow the data passing into the network to be relatively simpler. To account for differences in the model created by the altered data input, hyperparameter tuning was again implemented to reach the best accuracies and losses while keeping the architecture constant. Both segmentation methods used almost all the same hyperparameters after tuning, with the one exception being epochs as seen in Table 3.

The results for both the K-means clustering and SynthSeg segmentation processes with optimized hyperparameters are seen in Figures 8 and 9. For K-means clustering, the maximum validation

Table 3: Optimized Hyperparameters for both Segmentation Methods

	K-means clustering	SynthSeg
Graph Complexity	20	20
Batch Size	16	16
Hidden Channels	128	128
Threshold	0.6	0.6
Learning Rate	1e-3	1e-3
Epochs	30	24

accuracy was 89.47% with a validation loss of 0.178 while for SynthSeg, the maximum validation accuracy was 88.9% with a validation loss of 0.0044.

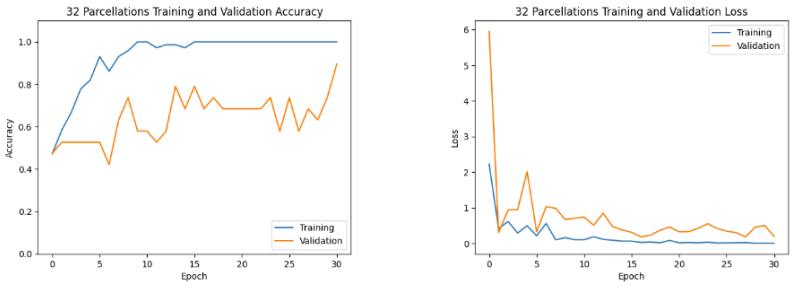

Figure 2: K-Means Clustering Segmentation Method Results

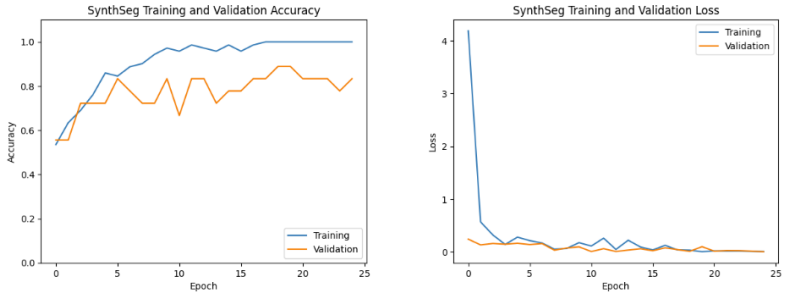

Figure 3: SynthSeg Segmentation Method Results

Since both segmentation methods yield similar results, they are viable graph network construction techniques, with SynthSeg producing slightly more favorable results. Additionally, considering differences in the accuracies and losses between Experiment 1 and this experiment, we conclude that less parcellations and nodes represent Parkinson's disease results better. This can be attributed to a less complex graph generated with fewer features coupled with a small training dataset that enables significantly improved performance compared to the baseline.

4.3 Literature Model Comparison

The previous two experiments demonstrated the optimized performance of a conventional GCN architecture modified and trained according to the characteristics of the functional connectivity associated with Parkinson's disease. However, the dataset and model chosen has no reference in literature and thus is limited in providing insight to what influences the performance of the GCN model. To overcome this, we implemented a residual GCN model from literature used to classify schizophrenia patients from fMRI images. The model shown in Figure 11 includes 3 hidden layers consisting of a graph convolutional layer with 128 channels and a top_k pooling operator whose residuals are added together and passed through a four layer perceptron for classification. After the first layer of the multilayer perceptron, a dropout regularization is applied and between each layer of

the multilayer perceptron, a batch normalization and ReLU activation function is applied. A sigmoid function is applied to the output to return binary prediction scores [9].

The reported hyperparameters acting as a baseline for this experiment for which over 92% accuracy in classifying schizophrenia was obtained are outlined in Table 4 For simplicity, we kept graph complexity at 20 and threshold at 0.6.

Table 4: Baseline Hyperparameters for Residual GCN Model

Loss Function	Cross Entropy Loss
Learning Rate	1e-4
Batch Size	10
Dropout Rate	0.5
Epochs	200

Figure 11 shows that the maximum validation accuracy achieved from training the residual model with the Parkinson's dataset with baseline hyperparameters was 57%. Since the validation loss increased past the point of convergence, the training was stopped early. When optimizing the model with the hyperparameters outlined in Table 5, we achieved 84% accuracy as shown in Figure 12.

Table 5: Optimized Hyperparameters for Residual GCN Model

Loss Function	Binary Cross Entropy Loss
Learning Rate	1e-3
Batch Size	64
Dropout Rate	0.8
Epochs	30

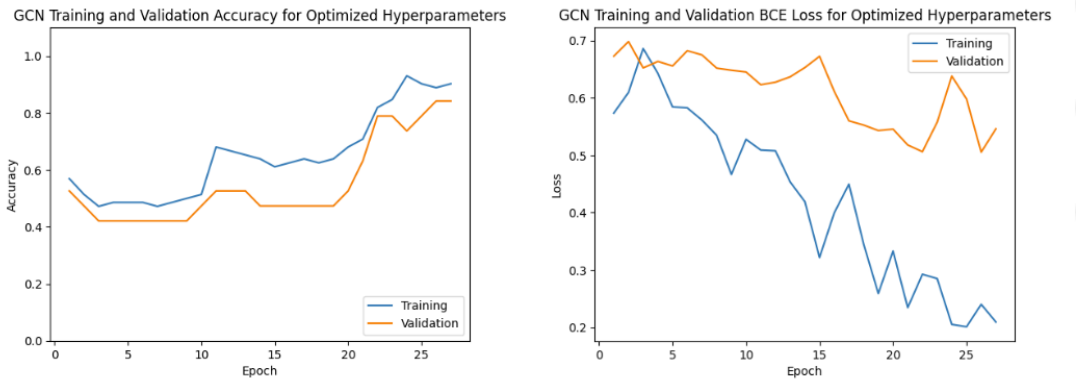

Figure 4: Training and Validation Performance with Optimized Literature Hyperparamaters

From the baseline validation accuracy curve, the established model's baseline parameter settings failed to generalize the dataset and derive a distinct pattern from the functional connectivity of Parkinson's patients. This observation paired with the increasing trend in training accuracy and decreasing trend in training loss indicate that the model is overfitting the training data. However, a larger dropout rate, batch size, and learning rate allowed us to decrease overfitting and improve the performance of the residual model compared to our initial model. A larger dropout regularization rate may denote that the functional connectivity of a Parkinson brain is more complex than a schizophrenia one. This further implies that the functional connectivity of different neurological disorders may exhibit uniquely varying complexities. As a result, further GCN models developed for neurotechnologies and computational methods must be able to adapt to the diverse characteristics of diseased functional connectivities. However, it is important to note that the schizophrenia study implemented a different fMRI image parcellation method and had over 300 patients in their dataset. Thus, increased regularization improving performance may instead be attributed to a smaller number of features and dataset.

5 Individual Contributions

Each member contributed equally to the project.

Aryan Agarwal contributed to designing and executing Experiment 3, writing the report, preparing the final presentation, and performing literature search.

Udit Iyengar contributed to the design and results for Experiment 1, writing the report, and preparing the final presentation.

Rommani Mondal contributed to the design and execution of Experiment 2, doing a literature search to understand how existing work addresses this problem, the written report, and preparing the final presentation.

References

[1] "Statistics." Parkinson's Foundation, Parkinson's Foundation, https://rb.gy/m15mn.

[2] "Parkinson's Disease." Parkinson's Disease Dementia, Alzheimer's Association, https://rb.gy/96vr0.

[3] Tolosa, E., Garrido, A., Scholz, S. W., & Poewe, W. (2021). Challenges in the diagnosis of Parkinson's disease. The Lancet. Neurology, 20(5), 385–397. https://doi.org/10.1016/S1474-4422(21)00030-2.

[4] Jalilianhasanpour R, Beheshtian E, Sherbaf G, Sahraian S, Sair HI. Functional Connectivity in Neurodegenerative Disorders: Alzheimer's Disease and Frontotemporal Dementia. Topics in Magnetic Resonance Imaging : TMRI. 2019 Dec; 28(6):317-324. DOI: 10.1097/rmr.0000000000000223. PMID: 31794504.

[5] Gadgil, S., Zhao, Q., Pfefferbaum, A., Sullivan, E. V., Adeli, E., & Pohl, K. M. (2021, June 29). Spatio-Temporal Graph Convolution for Resting-State fMRI Analysis. arxiv.org. Retrieved from https://arxiv.org/pdf/2003.10613v3.pdf.

[6] Billot, B., Greve, D. N., Puonti, O., Thielscher, A., Van Leemput, K., Fischl, B., Dalca, A. V., & Iglesias, J. E. (2023). Synthseg: Segmentation of brain MRI scans of any contrast and resolution without retraining. Medical Image Analysis, 86, 102789. https://doi.org/10.1016/j.media.2023.102789.

[7] Bessadok, A., Mahjoub, M. A., & Rekik, I. (2022, September 28). Graph Neural Networks in Network Neuroscience. arXiv.org. Retrieved from https://arxiv.org/abs/2106.03535.

[8] Thirion, B., Varoquaux, G., Dohmatob, E., & Poline, J.-B. (2014). Which fMRI clustering gives good brain parcellations? Frontiers in Neuroscience, 8. https://doi.org/10.3389/fnins.2014.00167

[9] Chen, X., Zhou, J., Ke, P., Huang, J., Xiong, D., Huang, Y., Ma, G., Ning, Y., Wu, F., & Wu, K. (2023). Classification of schizophrenia patients using a graph convolutional network: A combined functional MRI and Connectomics analysis. Biomedical Signal Processing and Control, 80, 104293. https://doi.org/10.1016/j.bspc.2022.104293.

[10] Trevor K. M. Day and Tara M. Madyastha and Peter Boord and Mary K. Askren & Nicholas J. Wapstra and Thomas J. Montine and Thomas J. Grabowski (2022). ANT: Healthy aging and Parkinson's disease. OpenNeuro. [Dataset] doi: doi:10.18112/openneuro.ds001907.v3.0.2.

[11] Gao, Ll., Wu, T. The study of brain functional connectivity in Parkinson's disease. Transl Neurodegener 5, 18 (2016). https://doi.org/10.1186/s40035-016-0066-0

[12] Tanglay, O., Dadario, N. B., Chong, E. H. N., Tang, S. J., Young, I. M., & Sughrue, M. E. (2023). Graph theory measures and their application to neurosurgical eloquence. Cancers, 15(2), 556. https://doi.org/10.3390/cancers15020556

Appendix

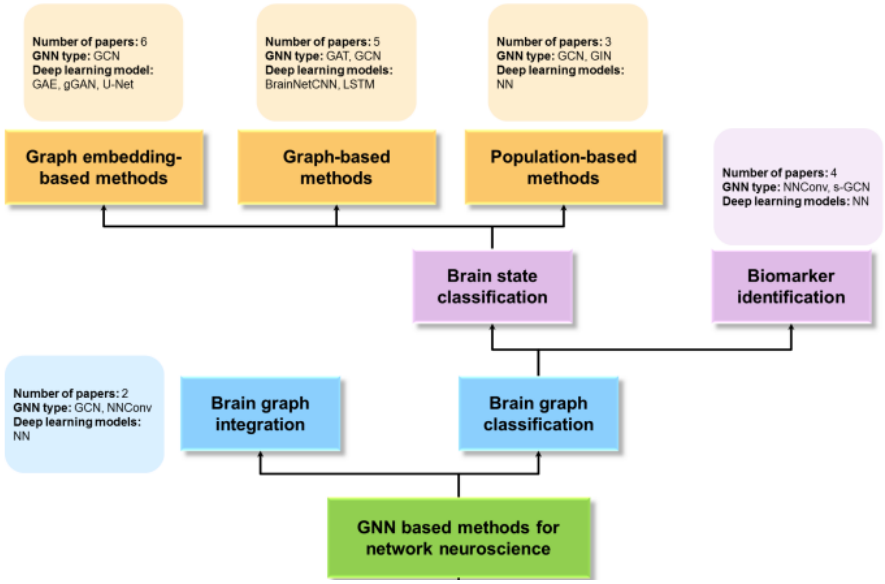

Figure 1: Literature landscape of GNN-based methods in neuroscience

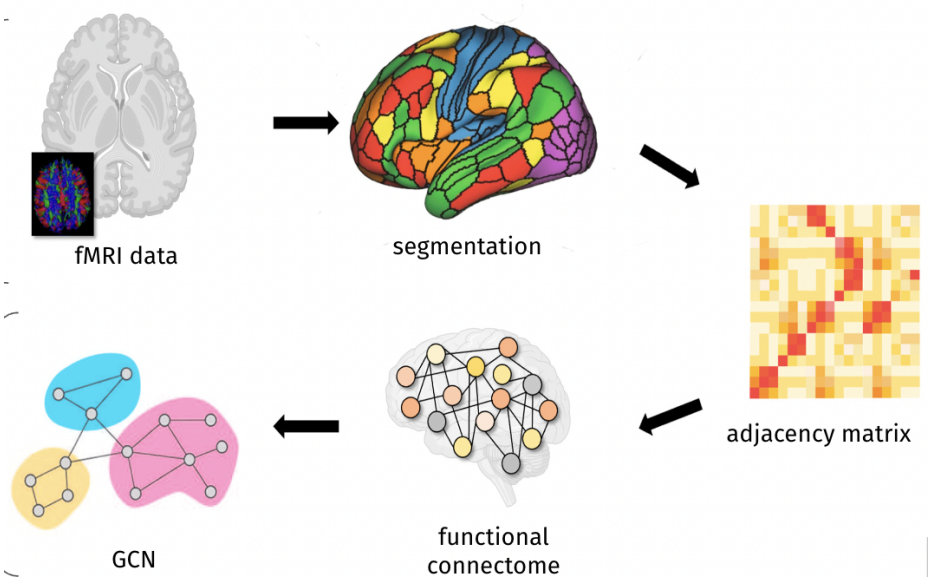

Figure 2: Diagram of Overall Disease Classification Process. Adapted from [12]

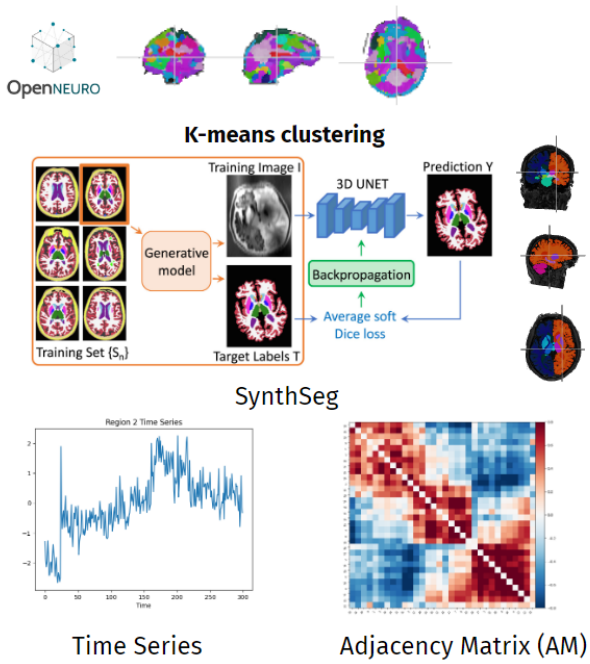

Figure 3: K-Means Clustering and SynthSeg Brain Segmentation Process

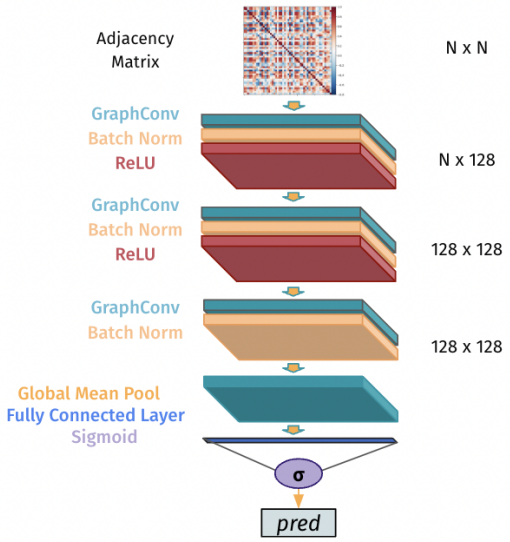

Figure 4: Graph Convolutional Network Model

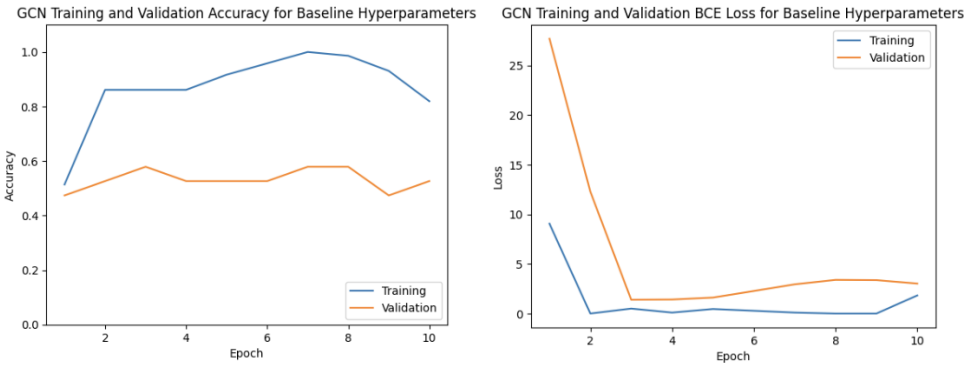

Figure 5: Training and Validation Performance with Baseline Model

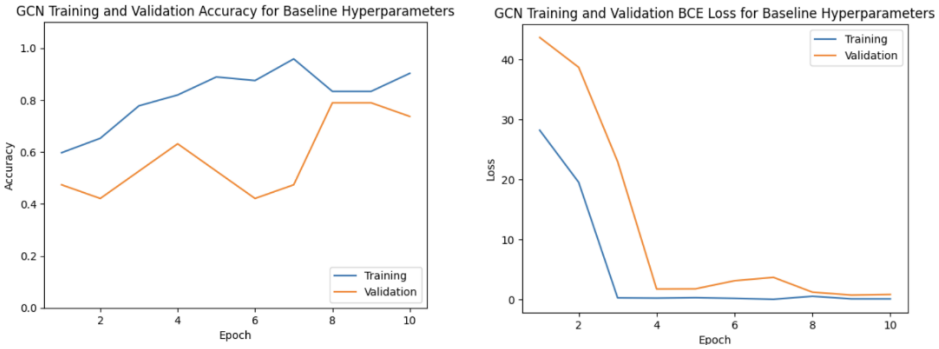

Figure 6: Training and Validation Performance with Optimized Architecture

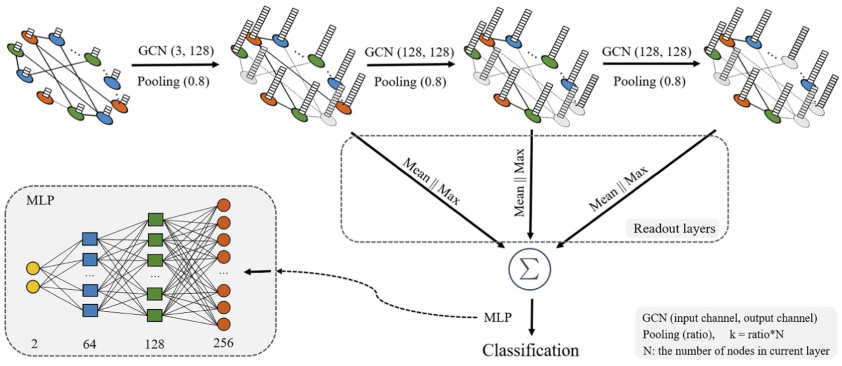

Figure 10: Baseline GCN Model Used for Classifying Schizophrenia [9]

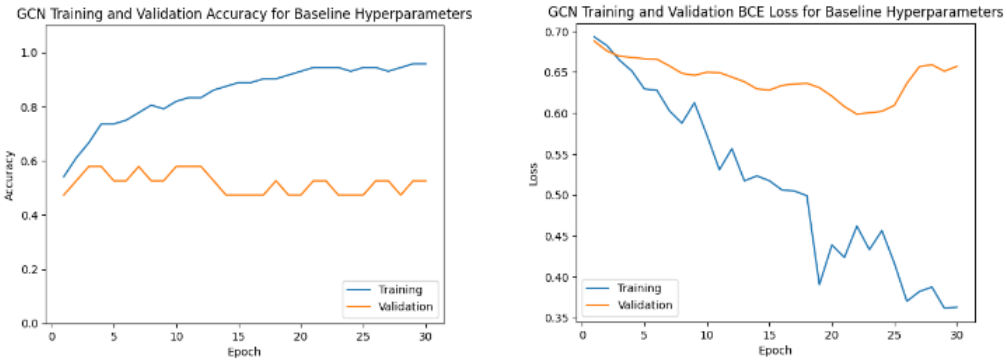

Figure 11: Training and Validation Performance with Baseline Literature Hyperparameters